Volume 17
Number 23
16 June 2026
Pages 2417-2532

Polymer Chemistry

rsc.li/polymers

ISSN 1759-9962

ROYAL SOCIETY OF CHEMISTRY

PAPER
Yosuke Akae *et al.*
Defining alternating sequences in polyurethanes: sequence-controlled photo-degradation in step polymerization

Polymer Chemistry

ROYAL SOCIETY OF CHEMISTRY

PAPER

View Article Online
View Journal | View Issue

Cite this: *Polym. Chem.*, 2026, **17**, 2423

Defining alternating sequences in polyurethanes: sequence-controlled photo-degradation in step polymerization

Xaver Kneidl,[a] Johannes Reeb-Begic,[a] Tongtong Cui,[a] Patrick Theato [a,b] and Yosuke Akae *†‡[a,c]

Programmable degradation is an important functionality for sustainable polymer materials; however, in conventional step polymerization of AA- and BB-type monomers, the polymer sequence itself has long lacked a clear and actionable definition. Polymers synthesized from AA- and BB-type monomers enable the incorporation of functional units directly into the polymer main chain, while inevitably featuring AA–BB connectivity; however, the concept of an "alternating" sequence has remained ambiguous. To address this fundamental limitation, we redefine sequence control in step polymerization by focusing on the connectivity unit rather than monomer composition. Using polyurethane as a representative model polymer, an AB-type monomer framework combined with dimeric species enables the explicit definition and practical implementation of (partially) alternating sequences. Incorporation of a photo-degradable monomer unit directly into the polymer backbone reveals pronounced sequence-dependent photo-degradability *via* main chain scission, which is drastically enhanced in alternating polymers, while thermal properties are likewise strongly influenced by polymer sequence. This work establishes the polymer sequence as an additional and actionable design parameter in polyurethanes as an example of step polymerization and provides a conceptual framework potentially applicable beyond polyurethanes to a broad range of AA/BB-based polymers. The utility of this framework for functional material development is demonstrated through sequence-controlled photo-degradation on the polymer main chain, offering a promising strategy toward sustainable polymer design.

Received 28th April 2026,
Accepted 13th May 2026

DOI: 10.1039/d6py00409a

rsc.li/polymers

Introduction

Controlling the polymer sequence is a fundamental challenge in polymer synthesis, essential both for understanding polymer primary structures and for enabling precise material design through tuning of properties such as degradability, recyclability, and mechanical performance.[1–30] Accordingly, extensive efforts have been devoted to achieving increasingly sophisticated sequence control across diverse polymer classes. However, these developments have been concentrated on chain polymerization processes, such as vinyl polymerization, where the concept of sequence is inherently well-defined, and functional units are typically incorporated into polymer side chains.

In contrast, step polymerization—despite its central importance in both academic and industrial polymer chemistry—has received limited attention from the perspective of sequence definition and control. Yet, many technologically relevant polymers, including polyesters, polyamides, polycarbonates, and polyurethanes (PUs), are synthesized *via* step-growth mechanisms. In these systems, typical polymers prepared from AA- and BB-type monomers inevitably exhibit AA–BB connectivity along the backbone. As a result, the concept of polymer sequence itself—and in particular, the meaning of an "alternating" sequence—remains ambiguous. This conceptual ambiguity has hindered systematic investigations of sequence–property relationships in polymers obtained by step polymerization, in sharp contrast to the well-established framework available for chain polymerization. While various advanced polymerization methods based on step polymerization have been developed, these approaches have largely focused on molecular weight control, leaving the polymer sequence inher-

[a]*Institute for Chemical Technology and Polymer Chemistry (ITCP), Karlsruhe Institute of Technology (KIT), 76131 Karlsruhe, Germany.*
E-mail: yosuke.akae@ac.rwth-aachen.de
[b]*Soft Matter Synthesis Laboratory – Institute for Biological Interfaces III (IBG-3), Karlsruhe Institute of Technology (KIT), 76344 Eggenstein-Leopoldshafen, Germany*
[c]*Research Fellow of Japan Society for the Promotion of Science, 102-0083 Tokyo, Japan*
†Present address: Department of Applied Chemistry, Graduate School of Engineering, The University of Osaka, 2-1 Yamadaoka, Suita, 565-0871 Osaka, Japan.
‡Present address: Institute of Inorganic Chemistry, RWTH Aachen University, Landoltweg 1a, 52074 Aachen, Germany.

ently ambiguous.[31–37] Because functional units are incorporated into the polymer main chain, sequence control in step polymerization provides a powerful tool for designing backbone-functional materials such as degradable polymers.

PU serves as a representative and industrially significant example of this issue.[38–56] Conventionally, PUs are synthesized *via* highly efficient polyaddition reactions between diols and di-isocyanates (Fig. 1A), allowing broad compositional flexibility and facile tuning of material properties ranging from soft elastomers to rigid coatings. Owing to their practical utility, most PU research has focused on formulation-driven material development rather than on precise control of the polymer primary structure. Nevertheless, it is evident that the positioning of urethane bonds and comonomer units along the polymer backbone critically influences thermal, mechanical, and functional properties, underscoring the importance of sequence control. However, conventional AA/BB-type polyaddition intrinsically lacks a framework to define or implement distinct sequence motifs, such as alternating arrangements, within PU backbones (Fig. 1A).

To address sequence control beyond conventional step polymerization, alternative PU production strategies have been explored. These include (i) ring-opening polymerization (ROP) of cyclic urethane monomers *via* chain-growth mechanisms and (ii) iterative one-by-one monomer addition to produce sequence-defined oligomers or polymers.[57–68] While these approaches have successfully enabled advanced structural control, they are associated with substantial synthetic cost and limited practicality. ROP approaches require multistep cyclic monomer synthesis and offer restricted structural diversity, whereas iterative synthesis suffers from high workload and typically limits accessible molecular weights to a few thousand g per mol or less. Consequently, a practical, scalable method that allows systematic sequence definition and control within the step polymerization framework remains highly desirable.

Recently, we introduced a facile PU synthesis strategy based on AB-type monomers, which provides a new platform to address this long-standing issue.[69–73] In this approach, monomers bearing both acyl azide and alcohol functionalities undergo heat-induced Curtius rearrangement to generate isocyanates *in situ*, triggering self-polyaddition between the isocyanate and alcohol groups (Fig. 1B). Because the acyl azide functionality is inert toward alcohols prior to the Curtius rearrangement, polymerization is effectively gated, enabling controlled step polymerization from AB-type building blocks. Importantly, this strategy establishes a clear definition of polymer sequence in PUs, enabling the construction of diverse polymer architectures, including block, statistical (random), grafted, and alternating polymers (Fig. 1C). The synthetic accessibility of AB-type monomers, readily derived from a diverse molecular pool of carboxylic acid species bearing alcohol groups, further allows flexible molecular design and broad monomer scope.

Using this framework, we have demonstrated that copolymerization behavior is strongly influenced by monomer reactivity, leading to statistical sequence distributions in certain systems. As expected, monomers featuring primary alcohol groups afford PUs more rapidly than those bearing secondary alcohol groups, resulting in statistical rather than completely random sequence distributions during copolymerization.[69–73] Moreover, this approach has enabled the preparation of functional PU materials with advanced primary structure control, including photo-degradable polymers. While earlier studies have reported PU synthesis from acyl azide–alcohol monomers, these efforts largely focused on homopolymer formation for bio-based materials or dendrimer synthesis, rather than on sequence definition or copolymerization.[74–77] Consequently, systematic implementation of alternating sequences within step polymerized PU backbones has remained unexplored.

Establishing a well-defined alternating sequence is particularly important for elucidating sequence–property relationships in step polymerization. To clearly evaluate the impact of sequence control, alternating monomer pairs should ideally exhibit distinct chemical or physical characteristics that enable unambiguous structural and property differentiation. In this context, we previously developed a photo-degradable PU monomer **M1** featuring an *o*-nitrobenzyl alcohol (*o*-NBA) unit, which displayed a certain homo-diad preference during copoly-

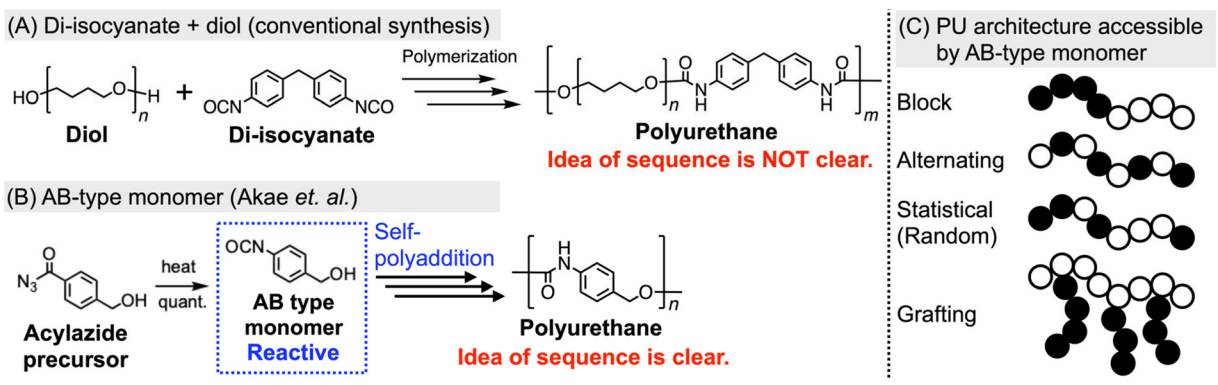

Fig. 1 General concept of this work as illustrated using PU as a model system; (A) PU synthesis by the conventional method; (B) PU synthesis based on the AB-type monomer featuring both acyl azide and alcohol groups;[69–73] (C) PU architectures accessible using the AB-type monomer.

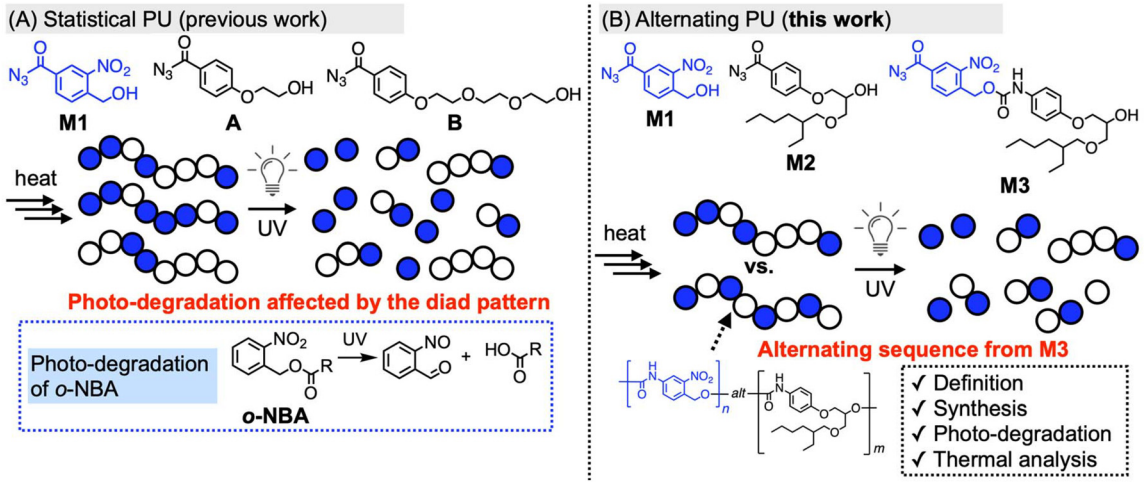

Fig. 2 Conceptual overview of PU sequence control using photo-degradable monomer **M1** in (A) previous work showing statistical sequence distribution;[72] (B) this work enabling alternating sequence incorporation.

merization (Fig. 2A).[72] This uneven monomer distribution led to inefficient photo-degradation due to the formation of locally concentrated photo-cleavable segments. Introducing an alternating sequence represents a rational strategy to homogenize the distribution of photo-degradable units and thereby enhance degradation efficiency. Furthermore, alternating incorporation of rigid **M1** units with flexible comonomers, such as **M2** bearing a 2-ethylhexyl side chain, is expected to significantly influence the thermomechanical properties of the resulting polymers (Fig. 2B).[73]

In this study, we define and implement alternating sequences within a step polymerization framework using polyurethane as a representative model system to achieve advanced photo-degradability control. While our previous statistical sequence system demonstrated that the sequence could be discussed in AB-type polyurethane synthesis, it did not allow the explicit implementation of alternating connectivity; this limitation is addressed in this work through a dimer-based strategy. Such explicit alternating control is essential for examining sequence–property relationships without ambiguity arising from statistical sequence distributions. A newly designed dimeric monomer **M3** is employed to introduce alternating connectivity in combination with AB-type monomers **M1**/**M2** (Fig. 2B). The resulting polymers are systematically analyzed in terms of photo-degradability and thermal properties to elucidate the effects of the sequence control. As shown in this study, by redefining the connectivity unit through a combination of AB-type monomers and a dimeric species, step polymerization is transformed from a process with an ambiguous sequence definition into a sequence-definable one. This work therefore establishes a conceptual and synthetic framework for defining and implementing alternating sequences in step polymerization, while sequence-dependent properties are examined as validation of its chemical and functional significance.

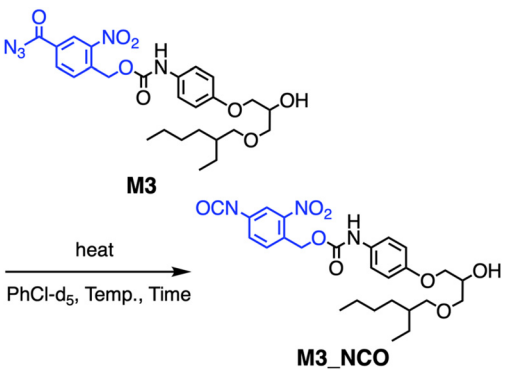

Scheme 1 Curtius rearrangement of **M3**.

Results and discussion

M1–**M3** were all synthesized by following previously reported standard synthesis including the final step to convert a carboxylic acid group into an acyl azide group using diphenyl phosphoryl azide (DPPA).[69–73,78–83] Newly synthesized **M3** was obtained as a solid at room temperature, the same as **M1**, while **M2** is liquid. According to previous results, liquid monomers typically show good polymerizability under bulk conditions, while solid ones often need some solvent during the polymerization for supplying enough fluidity to the reaction mixture, but this issue is affected by the T_g/T_m of the corresponding polymers. Since the polymerization behaviors of **M1** and **M2** were already investigated in previous studies, that of **M3** is first evaluated.

The kinetic analysis of the Curtius rearrangement of **M3** was studied by following previous reports (Scheme 1).[69–73,83–86] Namely, **M3** was dissolved in PhCl-d_5 at 0.020 M concentration and heated at 100 °C to induce the Curtius rearrangement. ^{1}H NMR measurements were conducted after 5, 10, and 15 min of

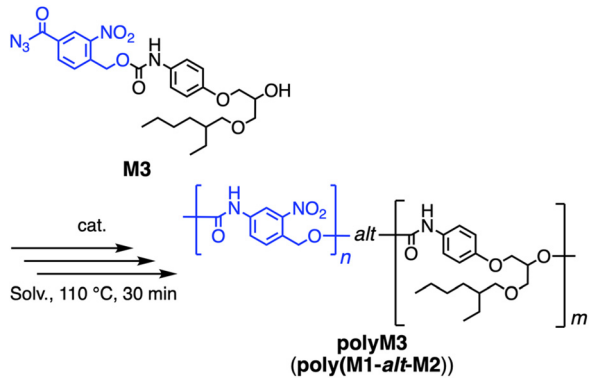

Scheme 2 Homopolymerization of **M3**.

heating to estimate the time-course of the spectral integration for calculating the kinetic constant. The results are summarized in the SI, and the obtained kinetic values are consistent with previous reports.[69–73] Namely, the Curtius rearrangement reaches a quantitative conversion within 60 min at 100 °C, and 30 min at 110 °C, which will be used for the setup of the polymerization conditions.

Next, to gain an insight into the polymerization behavior of **M3**, its homopolymerization was conducted under four standard reaction conditions (Scheme 2 and Table 1). Namely, the polymerization was carried out at 110 °C for 30 min in bulk or DMF (1.0 M) solvent, in the absence or presence of the dibutyltin dilaurate (DBTDL) catalyst, which was subsequently purified by precipitation to cold MeOH. The SEC profiles of products showed unimodal signals, while their ^{1}H NMR spectra clearly indicated the successful formation of **polyM3** (Fig. 3, 4A, and B).[83] Namely, ^{1}H NMR signals of the polymer became broader than the respective monomer signals, and each peak shift before and after the polymerization was consistent with previous reports,[69–73] while the generation of a new urethane signal e_1 at 10.4 ppm clearly indicated the occurrence of polymerization. Comparing the investigated four conditions (Table 1), the polymerization in bulk with the catalyst afforded the highest yield and the highest molecular weight (**polyM3a**, 59%, M_n = 11 kDa, and $Đ$ = 1.6), while other reaction conditions also successfully provided the desired polymer. Since the effective copolymerization conditions for **M1**/**M2**/**M3** would depend on the comonomer combination, the observed applicability of **M3** on various polymerization conditions is useful. Although the polymerization under DMF solution conditions without the catalyst resulted in a low yield (27%), the corresponding homopolymerization of **M2** only afforded a trace amount of **polyM2**,[73] suggesting the higher reactivity of **M3** than **M2** and/or the lower solubility in the precipitation solvent (cold MeOH) of the **polyM3** framework than that of **polyM2**. Since **polyM3** has the equivalent structure to **poly(M1-*alt*-M2)**, PU featuring the alternating sequence was successfully synthesized by step polymerization. For clarification, "alternating sequence", in this manuscript, refers to the strict alternating connection of **M1** and **M2** units provided by the

Table 1 Reaction conditions of the homopolymerization of **M3** presented in Scheme 2

Polymer	Solv.	DBTDL (cat.)	Yield [%]	M_n [a] [kDa]	M_w [a] [kDa]	$Đ$
polyM3a	Bulk	O	59	11	18	1.6
polyM3b	Bulk	X	49	9.6	16	1.7
polyM3c	DMF	O	52	9.2	15	1.8
polyM3d	DMF	X	27	7.8	12	1.5

[a] Calculated by SEC (eluent: DMAc, flow rate: 0.5 mL min^{-1}, and 50 °C).

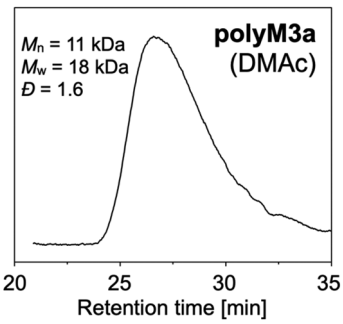

Fig. 3 SEC profile of **polyM3a** (eluent: DMAc, flow rate: 0.5 mL min^{-1}, and 50 °C).

dimeric monomer **M3**, distinguishing it from the inherent repeating unit alternation in traditional AA/BB polymerization.

To study the sequence-property control on various **M1**/**M2** feed ratios, copolymerization of **M1**, **M2**, and **M3** was conducted (Scheme 3 and Table 2). Here, the **M1**/**M2** feed ratio is set as 1/1, 4/1, and 1/4, and the alternating sequence was partially integrated by copolymerization with **M3** (Schemes 3B and C). In the case of high **M1** content, the DMF solution conditions were applied to promote effective polymerization, while the bulk conditions were applied for high **M2** content, considering the preferable polymerization conditions of **M1** and **M2**.[69–73] When **M1**/**M2** is 1/1, both the solution and the bulk conditions were applied (**poly(M1-*stat*-M2)a** and **poly(M1-*stat*-M2)d**). As a result, all the copolymers were successfully synthesized in moderate to high yields as confirmed by each unimodal SEC signal with M_n values of around 6–13 kDa.[83] All the ^{1}H NMR signals of the copolymer were clearly assigned in a similar manner to **polyM3**, which also indicated the successful polymer synthesis (Fig. 4C).[83] Interestingly, certain differences were observed in ^{1}H NMR signals between the alternating polymer **polyM3** and the **M1**/**M2** = 1/1 statistical copolymer **poly(M1-*stat*-M2)a** (Fig. 4B and C). In general, the statistical copolymer showed broader peaks than the alternating copolymer, which indicated a more diverse chemical status of the corresponding signals on the former. This broadening effect is consistent considering the existence of various sequence patterns on the statistical copolymer, while the alternating one has only a single pattern. Moreover, multiple aliphatic signals near urethane bonds showed two signals on the statistical

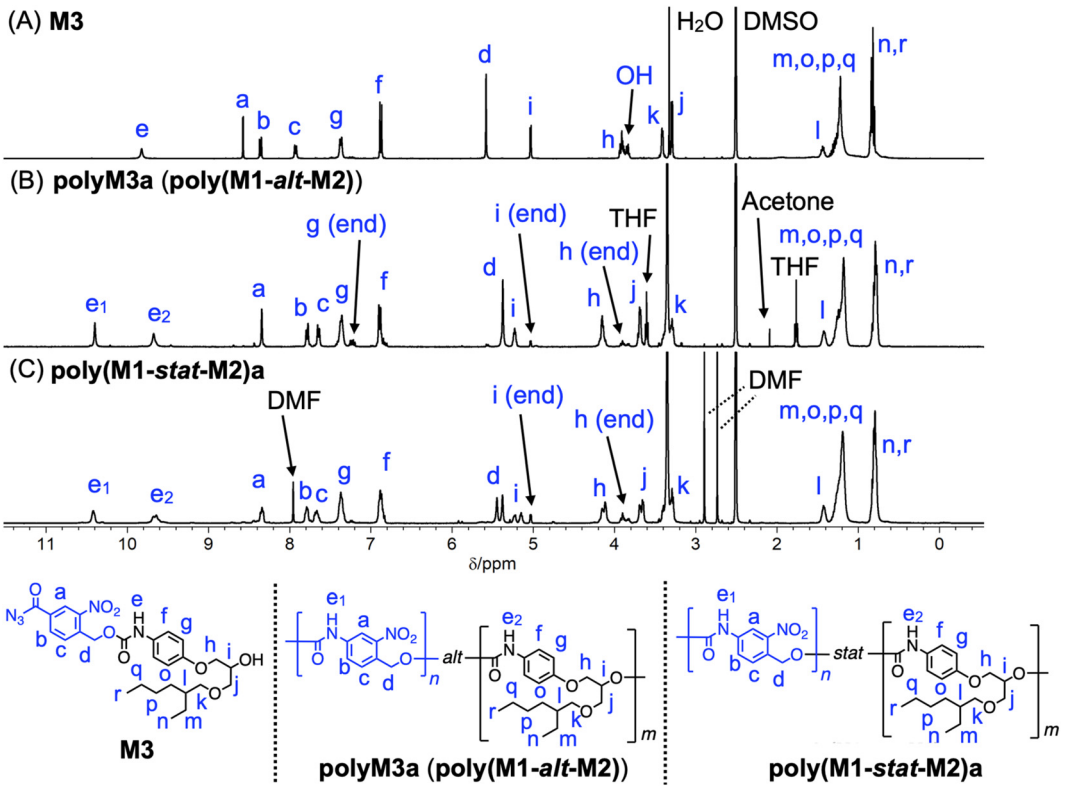

Fig. 4 ^{1}H NMR spectra of (A) **M3**; (B) **polyM3a** (**poly(M1-*alt*-M2)**); (C) **poly(M1-*stat*-M2)a** (400 MHz, 298 K, DMSO-d_6).

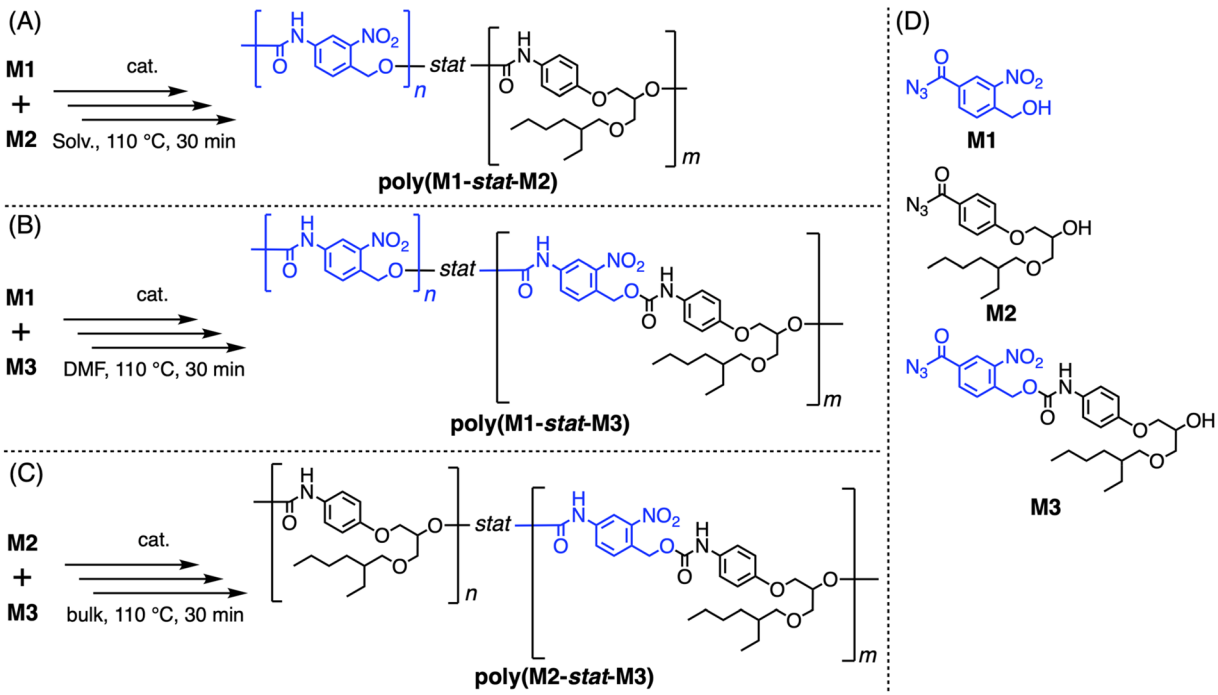

Scheme 3 Copolymerization of (A) **M1**/**M2**; (B) **M1**/**M3**; (C) **M2**/**M3**. (D) Chemical structures of **M1**–**M3**.

polymer, while only single signals were observed for the alternating copolymer, *e.g.* the benzyl proton of the **M1** unit *d* at 5.4 ppm and alkyl signals *h* at 4.2 ppm, *i* at 5.2 ppm, and *j* at 3.7 ppm of the **M2** unit. These equally split signals in the statistical copolymer are attributed to two different local diad environments, depending on whether the corresponding

Table 2 Copolymerization results shown in Scheme 3

Polymer	Monomer feed ratio	**M1**/**M2** unit feed ratio	Solv.	Composition[a] **M1**/**M2**	Yield [%]	M_n[b] [kDa]	M_w[b] [kDa]	$Đ$[b]
poly(M1-*stat*-M2)a	**M1**/**M2** = 1/1	1/1	DMF	49/51	65	8.6	12	1.3
poly(M1-*stat*-M2)b	**M1**/**M2** = 4/1	4/1	DMF	70/30	77	8.0	15	1.9
poly(M1-*stat*-M2)c	**M1**/**M2** = 1/4	1/4	bulk	22/78	29	6.0	10	1.7
poly(M1-*stat*-M2)d	**M1**/**M2** = 1/1	1/1	bulk	49/51	67	13	17	1.4
poly(M1-*stat*-M3)	**M1**/**M3** = 3/1	4/1	DMF	72/28	97	8.2	15	1.8
poly(M2-*stat*-M3)	**M2**/**M3** = 3/1	1/4	bulk	24/76	55	9.3	13	1.4

[a] Calculated from ^{1}H NMR spectra. [b] Calculated by SEC (eluent: DMAc, flow rate: 0.5 mL min^{-1}, and 50 °C).

repeating unit is next to **M1** or **M2**, which is also consistent with the previous observation on other PUs from AB-type monomers.[69–73] In contrast, the alternating copolymer provides only a single local sequence environment, resulting in one corresponding signal for each resonance. Thus, the sequence effect, statistical *vs.* alternating, was clearly observed in NMR measurement. The compositions of the obtained copolymers were calculated using ^{1}H NMR analyses and approximately followed the feed ratio as summarized in Table 2.[83] Meanwhile, further detailed analysis of diad or triad patterns based on NMR was difficult because the difference between them could not be clearly detected in our current system. Although the homopolymerization of **M1** did not proceed effectively under bulk conditions, its copolymerization with **M2** certainly worked at the **M1**/**M2** ratio = 1/1 or 1/4, suggesting that the **M2** unit provides sufficient fluidity for the effective reaction progress during the polymerization. Including homopolymer **polyM3** (= **poly(M1-*alt*-M2)**) in addition to these copolymers, PUs with multiple **M1**/**M2** compositions were successfully synthesized featuring a certain degree of the alternating sequence, which has been difficult to achieve by other existing synthetic methods.

Next, thermal properties of the obtained polymers were analyzed using DSC and TGA measurements (Table 3).[83] As previously observed, **polyM1** has a thermal self-immolative nature by the conjugative depolymerization path, including the decarboxylation step (Scheme 4),[70,72,87–89] leading to the lower T_{d5} values of copolymers containing a high **M1** content (around 145 °C) than the ones with a high **M2** content (around

Table 3 Thermal parameters of polymers. The values of **polyM1** and **polyM2** are cited from previous reports[72,73]

Polymer	Monomer feed ratio	**M1**/**M2** unit feed ratio	T_g[b] [°C]	T_{d5}[c] [°C]
polyM1	—	—	ND[a]	141
polyM2	—	—	42	272
polyM3a	—	1/1	78	245
poly(M1-*stat*-M2)a	**M1**/**M2** = 1/1	1/1	66	210
poly(M1-*stat*-M2)b	**M1**/**M2** = 4/1	4/1	107	144
poly(M1-*stat*-M2)c	**M1**/**M2** = 1/4	1/4	56	237
poly(M1-*stat*-M2)d	**M1**/**M2** = 1/1	1/1	78	246
poly(M1-*stat*-M3)	**M1**/**M3** = 3/1	4/1	87	147
poly(M1-*stat*-M3)	**M2**/**M3** = 3/1	1/4	40	238

[a] Not detected. [b] Estimated by DSC (2nd heating). [c] Estimated by TGA.

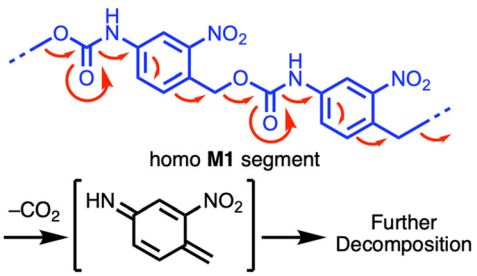

Scheme 4 Thermal degradation of the **M1** segment.

240 °C). Considering high T_{d5} values of **M1**/**M2** = 1/1 copolymers, the thermal degradation of the **polyM1** segment does not proceed effectively in these copolymers, probably because the **M2** unit stops the conjugative degradation path. Owing to the higher rigidity of the **M1** unit than **M2**, copolymers bearing the higher **M1** content generally showed higher T_g values, while certain differences were observed according to the sequence. A clear T_g difference was observed in **M1**/**M2** = 4/1 samples, **poly(M1-*stat*-M2)b** and **poly(M1-*stat*-M3)** (107 °C and 87 °C). In the latter, the soft **M2** unit is always located next to the **M1** unit through the alternating sequence, which effectively reduces the packing of the local homo-**M1** segment, while the generation of a certain amount of homo-**M1** or **M2** segments is inevitable in the former, which could induce easier homo-segment packing to increase the T_g value (Fig. 5). A similar T_g difference was observed in **M1**/**M2** = 1/4 samples, **poly(M1-*stat*-M2)c** and **poly(M2-*stat*-M3)** (56 °C and 40 °C), which can be explained in the same manner. Namely, the dimer integration induced the distribution of the hard **M1** unit always next to the soft **M2** unit, while the generation of a certain content of homo-**M1**/**M2** was inevitable in the copolymerization without the dimer **M3**, which caused the trend of easier packing by local homo-polymer segments to increase the T_g value. In these cases, the partial alternating sequence (**M3** unit) introduction significantly reduced the packing nature of the local polymer segments compared with the corresponding statistical copolymers, resulting in the decrease of T_g values. Meanwhile, the reason for the difference in T_g values between **M1**/**M2** = 1/1 statistical polymers (**poly(M1-*stat*-M2)a** and **poly(M1-*stat*-M2)d**) was not completely clear, but could have been influenced by the sequence formation process during the polymerization. Namely, the bulk conditions used

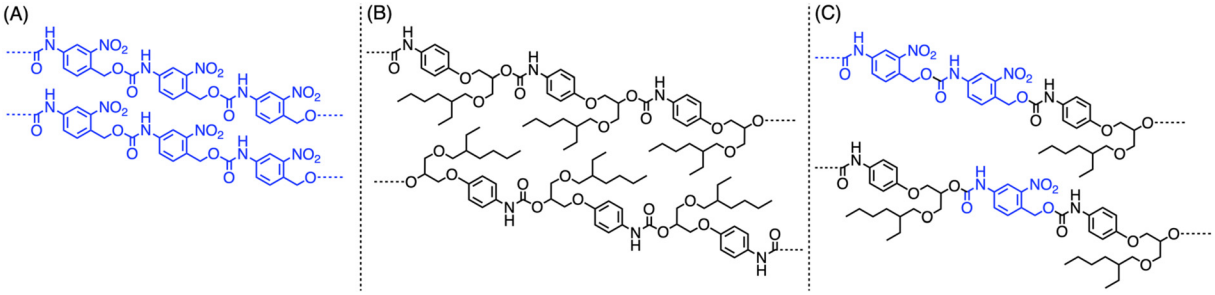

Fig. 5 Schematics of the plausible local polymer packing structure of (A) the homo-**M1** segment; (B) homo-**M2** segment; (C) **M1**/**M2** hetero-segment.

for **poly(M1-*stat*-M2)d** reduced the fluidity of the polymerization mixture during the copolymerization, which would have caused the local homo-**M1**/**M2** segment formation, while the DMF solution conditions used for **poly(M1-*stat*-M2)a** induced a more homogeneous distribution of **M1**/**M2** units in the polymer framework. The resulting sequence difference would have caused the different T_g values. Interestingly, **poly(M1-*stat*-M3)** having a 20% hard **M1** content showed a slightly lower T_g value than the 100% soft segment homopolymer **polyM2** (40 °C and 42 °C respectively). This suggested that the small content of **M1** on the former disturbed the effective packing of the aliphatic side chain moieties of the entire **polyM2** framework to reduce T_g, and this effect would work more dominantly than the increase of the rigidity by the introduction of the hard **M1** unit. Considering the above discussion about the polymer sequence, the implementation of the alternating sequence was clearly proved to affect the thermal properties of the polymer derived from step polymerization (PU in this case), underscoring the importance of the "sequence" as a parameter to control the basic properties of the polymer obtained by step polymerization. Moreover, the pronounced sequence dependence observed in thermal properties indicates that the sequence effect is not limited to photo-cleavable systems, although photo-degradability was chosen in this work as a particularly clear model response.

Next, the photo-degradability of copolymers was investigated to evaluate the effect of their sequences on it by following the previous report (Fig. 6 and 7 and Scheme 5).[72] Namely, each copolymer was dissolved in THF or DMAc under diluted conditions (1 mg mL^{-1}), and 365 nm light was irradiated to induce the photo-cleavage reaction of the *o*-NBA framework on the **M1** unit, which was traced by SEC measurements after 0, 5, 10, 15, 30, 60, and 120 min of light irradiation and summarized as a time-course M_n plot (Fig. 7). Here, the result of the THF system is discussed, because the result of DMAc indicated a similar trend, and the former showed sharper SEC signals that could be clearly detected.[83] First, all the samples showed a clear decrease in the molecular weight even after 5 min of irradiation, and the continuous irradiation induced a further decrease that was mostly completed within one hour, while the control test of UV irradiation on **polyM2** did not change its SEC profile at all even after several hours, clearly indicating the occurrence of photo-degradation in the **M1** unit.[83] The general trend of the photo-degradability is consistent with the previous report,[72] indicating that copolymers bearing a high **M1** content are likely to show more intensive photo-degradability, while certain effects of the sequence were clearly observed as discussed in the following.

Comparing **polyM3a** and **polyM3c**, both of which feature the alternating sequence **poly(M1-*alt*-M2)**, the former showed more intensive degradation than the latter. Since both polymers have the same sequence/composition, this difference would be caused by the molecular weight difference. In this method, the minimum unit after the photo-degradation is the monomeric unit from **M1** (M_w ~ 150 Da) or the dimeric unit from the **M2**–**M1** diad (M_w ~ 470 Da), indicating that the size of the initial polymer certainly affects the percentage of the M_n decrease when it is around 10 kDa or less. Thus, the initially bigger **polyM3a** (M_n = 8.4 kDa) showed a greater decrease in the percentage of M_n from the beginning to the complete degradation than **polyM3c** (M_n = 5.2 kDa). It also affects the more intensive degradation of **polyM3a** than the copolymers bearing an 80% **M1** content (**poly(M1-*stat*-M3)** and **poly(M1-*stat*-M2)b**). In this case, the high **M1** content increases the photo-degradability of polymers, but it also causes a lower molecular weight in the resulting polymer, possibly because of the high rigidity of the **M1** unit,[72] which could cause low fluidity during the polymerization, hindering the propagation reaction. The effect of the molecular weight would be more dominant than the high content of the **M1** unit and would have induced the highest photo-degradability of **polyM3a** in this measurement. Except for **polyM3a**, copolymers bearing more than 50% **M1** content showed a similar trend in the time-course of the M_n decrease regardless of their sequence or the **M1** content, suggesting that these parameters do not significantly influence their photo-degradability, possibly because they are already highly photo-degradable. Meanwhile, a large photo-degradability difference was observed in copolymers bearing a 20% **M1** content (**poly(M2-*stat*-M3)** and **poly(M1-*stat*-M2)c**), the smallest **M1** content in this work. Both degraded less than the others, but **poly(M2-*stat*-M3)** (~45% decrease of M_n) degraded substantially less than **poly(M1-*stat*-M2)c** (~70% decrease of M_n), which was associated with the sequence difference. Namely, the alternating sequence from

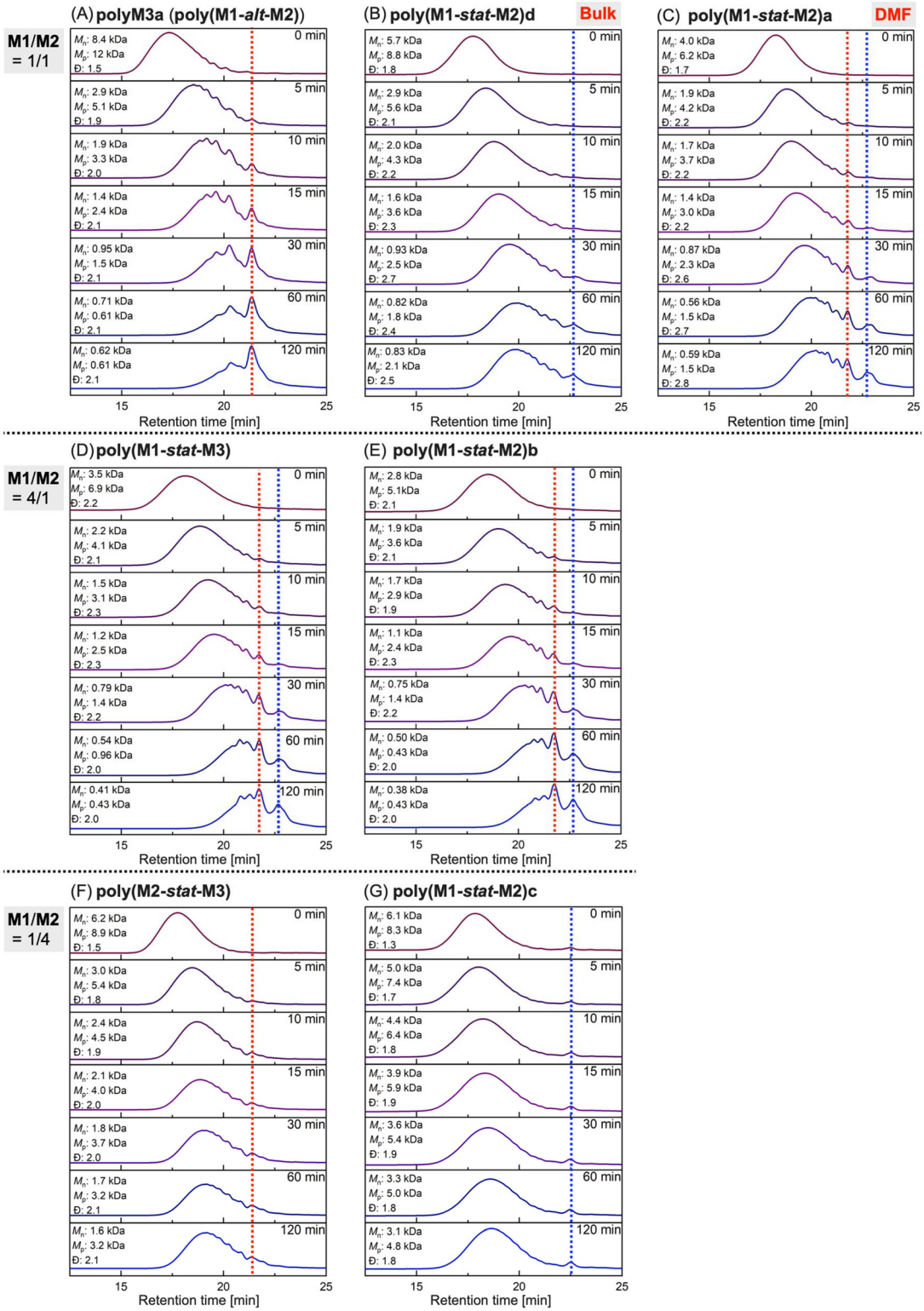

Fig. 6 Time course of SEC profiles of (A) **polyM3a**; (B) **poly(M1-*stat*-M2)d**; (C) **poly(M1-*stat*-M2)a**; (D) **poly(M1-*stat*-M3)**; (E) **poly(M1-*stat*-M2)b**; (F) **poly(M2-*stat*-M3)**; (G) **poly(M1-*stat*-M2)c** (UV irradiation for 0, 5, 10, 15, 30, 60, and 120 min; eluent: THF, flow rate: 1.0 mL min^{-1}, and 25 °C). The red dotted line indicates the dimeric fragment generation, while the blue one indicates the monomeric fragment.

M3 induces more homogeneous distribution of photo-degradable **M1** units in the entire polymer chain, while the **M1**/**M2** statistical polymer without **M3** includes inevitable local homo-**M1** and **M2** polymer segments, which decrease the photo-degradability owing to the non-photo-degradable homo-**M2** segment. When the **M1** content is higher than 50%, this effect

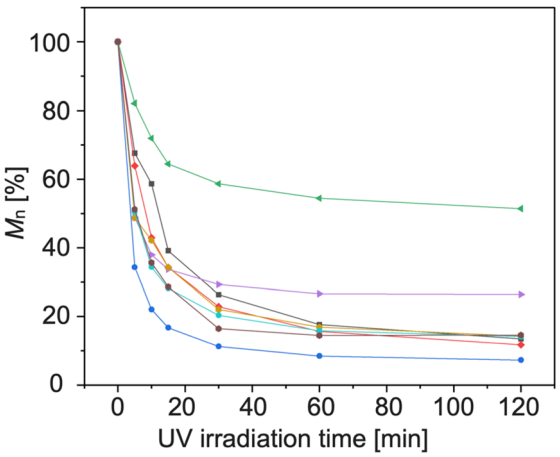

	M1/M2 unit ratio	M_n [kDa]
polyM3a	1/1	8.4
polyM3c	1/1	5.2
poly(M1-*stat*-M2)a	1/1	4.0
poly(M1-*stat*-M2)d	1/1	5.7
poly(M1-*stat*-M3)	4/1	3.5
poly(M1-*stat*-M2)b	4/1	2.8
poly(M2-*stat*-M3)	1/4	6.2
poly(M1-*stat*-M2)c	1/4	6.1

Fig. 7 Plot of M_n [%] *vs.* UV irradiation time of copolymers. The column of M_n shows the initial M_n before UV irradiation (eluent: THF, flow rate: 1.0 mL min^{-1}, and 25 °C).

would not be dominant, but it has a significant influence on the low **M1** content copolymers, resulting in a drastic photo-degradability difference between the partially alternating polymer and the complete statistical polymer. This "alternating *vs.* statistical" sequence-dependent photo-degradability was first observed by the implementation of sequence definition/control on the polymer derived from step polymerization (PU in this case), supporting its importance.

Meanwhile, SEC profiles showed further dependence of the resulting residues from the photo-degradation on the sequence (Fig. 6). According to the photo-degradation of **polyM3a**, the SEC intensity around 21.5 min (red dotted line in Fig. 6A) increased, suggesting the formation of dimeric fragments after the alternating polymer framework cleavage. The peaks at the same retention time were also observed on other polymers containing an alternating sequence (Fig. 6D and F). On the other hand, copolymers made from **M1** show an SEC peak increase around 22.5 min in proportion to the UV irradiation time (blue dotted lines in Fig. 6), which would be derived from the monomeric fragment after the photo-degradation of the homo-**M1** segment. Statistical polymers without **M3** integration also showed peaks from dimeric fragments around 21.5 min, suggesting the existence of various sequence patterns there, including the homo-**M1** segment and other hetero-segment types. Comparing two copolymers featuring 20% **M1** content, the one with the alternating sequence showed an intense dimeric fragment peak on the residue (Fig. 6F), while the one without the alternating sequence exhibited an intense monomeric fragment peak (Fig. 6G), highlighting the sequential difference and the homo-**M1** segment formation in **poly(M1-*stat*-M2)c**, which induced its more decreased photo-degradability and higher T_g than its partially alternating sequenced counterpart **poly(M2-*stat*-M3)**. Finally, comparing two statistical copolymers featuring **M1**/**M2** = 1/1 content, the one made in DMF solution showed a more intensive dimeric peak (Fig. 6C) than the one made in the bulk (Fig. 6B), while both showed monomeric fragment peaks. This difference is probably because the solvent increased the fluidity of the reaction mixture to induce a more homogeneous polymerization system, while the bulk conditions could cause the local aggregation of the homopolymer segments, resulting in monomeric fragment generation through photo-degradation and higher T_g due to their higher packing preference. Further spectroscopic analysis of the degradation products would provide deeper mechanistic insight into this system, but such analysis was experimentally difficult for the present degraded samples owing to the low product amount in diluted solution. Therefore, the degradation mechanism proposed here remains partly speculative and should be interpreted with appropriate caution. A more detailed structural elucidation of the degradation products will be the subject of future study.

Considering the above, the thermal properties and photo-degradability of **M1**/**M2** copolymers were consistently associated

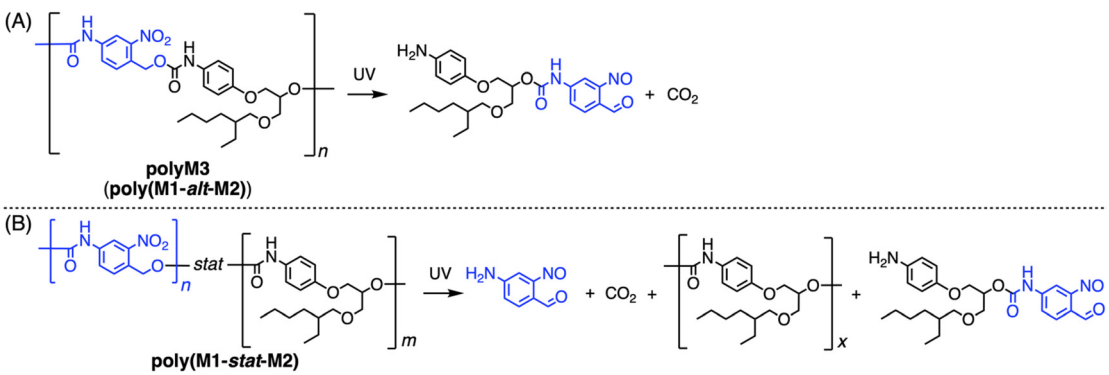

Scheme 5 Photo-degradation of (A) **polyM3** (**poly(M1-*alt*-M2)**) and (B) **poly(M1-*stat*-M2)**.

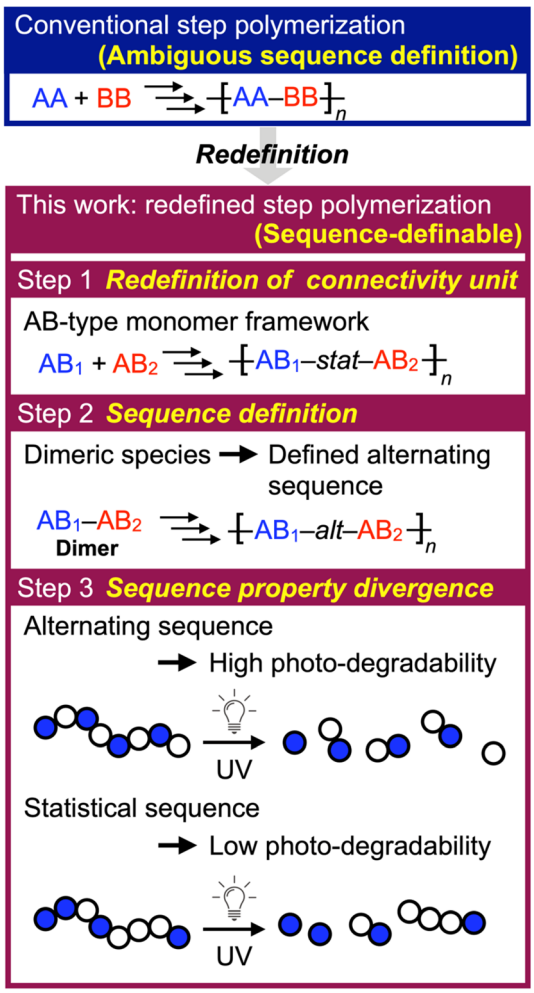

Fig. 8 Sequence definition of the polymer derived from step polymerization demonstrated in this work, highlighting the resulting sequence–property divergence for photo-degradation control.

with their polymer sequence, which was clearly controlled by the (partial) integration of the alternating sequence. The detailed analysis indicated a certain level of sequence-property control through the polymerization conditions (bulk *vs.* solution), which could supportively contribute to the polymer design. In the end, this work successfully demonstrated the definition of an alternating sequence in the polymer derived from step polymerization conventionally featuring only AA–BB-type connectivity by the combination of an AB-type monomer framework and the dimeric species, and the property analysis of redefined polymers suggested that the polymer sequence acts as an independent design parameter in step polymerization, giving rise to pronounced sequence-property divergence (Fig. 8).

Conclusion

In this work, we addressed a fundamental yet ambiguous question in step polymerization by defining what constitutes an alternating sequence in polymers synthesized from AA- and BB-type monomers. An AB-type monomer framework enabled explicit sequence definition, while a dimer-based strategy allowed the practical implementation of alternating connectivity. Using polyurethane as a model system, we demonstrated that defined alternating sequences give rise to pronounced sequence–property relationships, as reflected in thermal properties and photo-degradability, enabling programmable material degradation. The main contribution of this study is the establishment of a conceptual and synthetic basis for alternating sequences in step polymerization, while the observed sequence-dependent properties confirm the practical relevance of this framework. This study establishes polymer sequence as an additional and actionable design parameter in polyurethane as a model system for step polymerization, beyond conventional monomer and composition design. The framework demonstrated in this work would potentially be applicable to other step polymerization systems. By enabling the controlled incorporation of the functional unit into the polymer main chain rather than the side chain, this method provides a complementary tool for contributing to functional/sustainable material development other than well-studied chain polymerization.

Author contributions

X. K.: data curation, formal analysis, investigation, and visualization; J. R.-B.: data curation and investigation; T. C.: data curation; P. T.: resources and writing – review & editing; Y. A. conceptualization, formal analysis, funding acquisition, methodology, project administration, resources, supervision, validation, visualization, writing – original draft, and writing – review & editing.

Conflicts of interest

The authors declare no conflicts of interest.

Data availability

The data supporting this article have been included as part of the supplementary information (SI). Supplementary information (SI): general methods, chemical synthesis, property analysis of the synthesized compounds, kinetic analysis, and spectra of the synthesized compounds. See DOI: https://doi.org/10.1039/d6py00409a.

Acknowledgements

This work was supported by JSPS KAKENHI (Japan) grant numbers JP20J00360 (Y. A.), JP21K14672 (Y. A.), and JP22KJ1489 (Y. A.). The authors acknowledge financial support from the Helmholtz Association.

References

1 J. F. Lutz, M. Ouchi, D. R. Liu and M. Sawamoto, Sequence-Controlled Polymers, *Science*, 2013, **341**, 1238149.
2 S. L. Perry and C. E. Sing, 100th Anniversary of Macromolecular Science Viewpoint: Opportunities in the Physics of Sequence-Defined Polymers, *ACS Macro Lett.*, 2020, **9**, 216–225.
3 Q. Shia, Z. Denga, M. Houa, X. Hua and S. Liu, Engineering precise sequence-defined polymers for advanced functions, *Prog. Polym. Sci.*, 2023, **141**, 101677.
4 M. A. R. Meier and C. Barner-Kowollik, A New Class of Materials: Sequence-Defined Macromolecules and Their Emerging Applications, *Adv. Mater.*, 2019, **31**, 1806027.
5 Z. Gan, J. Liu, Z. Xu, S. Jia and X.-H. Dong, Precision polymers: advances in synthesis, structural engineering, and functional optimization, *Prog. Polym. Sci.*, 2025, **170**, 102030.
6 L. D. Thai, J. A. Kammerer, D. Golberg, H. Mutlu and C. Barner-Kowollik, Sequence-defined main-chain photoswitching macromolecules with odd-even effect-controlled properties, *Chem*, 2025, **11**, 102341.
7 H. S. Wang, M. Agrachev, H. Kim, N. P. Truong, T.-L. Choi, G. Jeschke and A. Anastasaki, Visible Light–Triggered Depolymerization of Commercial Polymethacrylates, *Science*, 2025, **387**, 874–880.
8 L. Cederholm, P. Olsen, M. Hakkarainen and K. Odelius, Design for Recycling: Polyester- and Polycarbonate-Based A–B–A Block Copolymers and Their Recyclability Back to Monomers, *Macromolecules*, 2023, **56**, 3641–3649.
9 Y. Takahashi, A. Kanazawa and S. Aoshima, 3-Alkoxyphthalides as Nonhomopolymerizable, Highly Reactive Comonomers for ABC Pseudo-Periodic Terpolymers and Degradable Polymers via Cationic co- and Terpolymerizations With Oxiranes and/or Vinyl Ethers, *Macromolecules*, 2023, **56**, 4198–4207.
10 M. Uchiyama, Y. Murakami, K. Satoh and M. Kamigaito, Synthesis and Degradation of Vinyl Polymers with Evenly Distributed Thioacetal Bonds in Main Chains: Cationic DT Copolymerization of Vinyl Ethers and Cyclic Thioacetals, *Angew. Chem., Int. Ed.*, 2023, **62**, e202215021.
11 Y. Xia, T. Shao, Y. Sin, J. Wang, C. Gu, C. Zhang and X. Zhang, Precise Placement of Thioester Bonds Into Sequence-Controlled Polymers Containing ABAC-type Units, *Nat. Commun.*, 2025, **16**, 1974.
12 Y. Akae and P. Theato, Aggregation Behavior of Cyclodextrin- Based [3]Rotaxanes, *Chem. – Eur. J.*, 2023, **29**, e202301582.
13 M. Uchiyama, M. Imai and M. Kamigaito, Synthesis of Degradable Polymers via 1,5-Shift Radical Isomerization Polymerization of Vinyl Ether Derivatives With a Cleavable Bond, *Polym. J.*, 2024, **56**, 359–368.
14 Y. Akae, Cyclodextrin-Based Rotaxanes for Polymer Materials: Challenge on Simultaneous Realization of Inexpensive Production and Defined Structures, *Beilstein J. Org. Chem.*, 2024, **20**, 3026–3049.
15 H. G. Hester, Z. B. A. Abel and G. W. Coates, Ultra-High-Molecular- Weight Poly(Dioxolane): Enhancing the Mechanical Performance of a Chemically Recyclable Polymer, *J. Am. Chem. Soc.*, 2023, **145**, 8800–8804.
16 Y. Akae and T. Takata, O-Acylative Vinylation of Cyclodextrin- Based [3]Rotaxane Towards Rotaxane Crosslinkers, *Eur. J. Org. Chem.*, 2023, **26**, e202300009.
17 A. Tardy, J. Nicolas, D. Gigmes, C. Lefay and Y. Guillaneuf, Radi- cal Ring-Opening Polymerization: Scope, Limitations, and Application to (Bio)degradable Materials, *Chem. Rev.*, 2017, **117**, 1319–1406.
18 H. Sogawa, C.-G. Wang, S. Monjiyama, Y. Akae and T. Takata, Aliphatic Ditopic Nitrile N-Oxide Crosslinker: Synthesis, Chemical Stability, and Catalyst-Free Crosslinking Reactions, *Polymer*, 2021, **213**, 123291.
19 C. Weng, X. Li and X. Tang, Solvent-Dependent Sequence-Controlled Copolymerization of Lactones: Tailoring Material Properties from Robust Plastics to Tough Elastomers, *Angew. Chem., Int. Ed.*, 2025, **64**, e202415388.
20 R. D. Rittinghaus, J. Zenner, A. Pich, M. Kol and S. Herres-Pawlis, Master of Chaos and Order: Opposite Microstructures of PCL-co-PGA-co-PLA Accessible by a Single Catalyst, *Angew. Chem., Int. Ed.*, 2022, **61**, e202112853.
21 M. Uchiyama, Y. Murakami, K. Satoh and M. Kamigaito, Synthesis and Degradation of Vinyl Polymers with Evenly Distributed Thioacetal Bonds in Main Chains: Cationic DT Copolymerization of Vinyl Ethers and Cyclic Thioacetals, *Angew. Chem., Int. Ed.*, 2023, **62**, e202215021.
22 T. Kimura, K. Kuroda, H. Kubota and M. Ouchi, Metal-Catalyzed Switching Degradation of Vinyl Polymers via Introduction of an "In-Chain" Carbon−Halogen Bond as the Trigger, *ACS Macro Lett.*, 2021, **10**, 1535–1539.
23 Y. Akae, H. Sogawa and T. Takata, Cyclodextrin Based [3] Rotaxane Crosslinked Fluorescent Polymer: Synthesis and De Crosslinking Using Size Complementarity, *Angew. Chem., Int. Ed.*, 2018, **57**, 14832–14836.
24 K. Watanabe, N. Kaizawa, B. J. Ree, T. Yamamoto, K. Tajima, T. Isono and T. Satoh, One-Shot Intrablock Cross-Linking of Linear Diblock Copolymer to Realize Janus-Shaped Single-Chain Nanoparticles, *Angew. Chem., Int. Ed.*, 2021, **60**, 18122–18128.
25 J. J. Lessard, G. M. Scheutz, S. H. Sung, K. A. Lantz, T. H. Epps III and B. S. Sumerlin, Block Copolymer Vitrimers, *J. Am. Chem. Soc.*, 2020, **142**, 283–289.
26 M. Appold, C. Mari, C. Lederle, J. Elbert, C. Schmidt, I. Ott, B. Stühn, G. Gasser and M. Gallei, Multi-stimuli responsive block copolymers as a smart release platform for a polypyridyl ruthenium complex, *Polym. Chem.*, 2017, **8**, 890–900.
27 Y. Akae, Y. Koyama, H. Sogawa, Y. Hayashi, S. Kawauchi, S. Kuwata and T. Takata, Structural Analysis and Inclusion Mechanism of Native and Permethylated α-Cyclodextrin-Based Rotaxanes Containing Alkylene Axles, *Chem. – Eur. J.*, 2016, **22**, 5335–5341.
28 K. Satoh, D.-H. Lee, K. Nagai and M. Kamigaito, Precision Synthesis of Bio-Based Acrylic Thermoplastic Elastomer by

RAFT Polymerization of Itaconic Acid Derivatives, *Macromol. Rapid Commun.*, 2014, **35**, 161–167.
29 Y. Akae, T. Arai, Y. Koyama, H. Okamura, K. Johmoto, H. Uekusa, S. Kuwata and T. Takata, One-Pot Synthesis of Permethylated α-CD-Based Rotaxanes Having Alkylene Chain Axles and Their Structural Characteristics, *Chem. Lett.*, 2012, **41**, 806–808.
30 J. Li, R. M. Stayshich and T. Y. Meyer, Exploiting Sequence to Control the Hydrolysis Behavior of Biodegradable PLGA Copolymers, *J. Am. Chem. Soc.*, 2011, **133**, 6910–6913.
31 A. Ravve, Step-Growth Polymerization and Step-Growth Polymers, in *Principles of Polymer Chemistry*, Springer, New York, 2012, pp. 403–535.
32 M. Ueda, K. Kimura and T. Yokozawa, Polycondensation, in *Polymer Synthesis*, ed. T. Endo, Kodansha, Tokyo, 2010, pp. 569–744.
33 T. Yokozawa and Y. Ohta, Transformation of Step-Growth Polymerization into Living Chain-Growth Polymerization, *Chem. Rev.*, 2016, **116**, 1950–1968.
34 A. Yokoyama and T. Yokozawa, Converting Step-Growth to Chain-Growth Condensation Polymerization, *Macromolecules*, 2007, **40**, 4093–4101.
35 S. Sakai, T. Nakamura, S. Uchida, Y. Nakauchi, M. Uchiyama, T. Kubo, M. Kamigaito and K. Satoh, Controlled/Living Click Polymerization with Possible Bidirectional Chain-Growth Propagation during Polyaddition, *J. Am. Chem. Soc.*, 2025, **147**, 21459–21467.
36 J. Yang, L. Chen, M. Zhu, M. W. Ishaq, S. Chen and L. Li, Investigation of the Multimer Cyclization Effect during Click Step- Growth Polymerization of AB-Type Macromonomers, *Macromolecules*, 2022, **55**, 6830–6840.
37 R. Ejima, M. Nakahata, Y. Kamon and A. Hashidzume, Synthesis and Metal Ion Adsorption Properties of a Dense Triazole Polymer Carrying Cysteine Residues, *J. Polym. Sci.*, 2025, **63**, 1570–1579.
38 E. Delebecq, J. P. Pascault, B. Boutevin and F. Ganachaud, On the Versatility of Urethane/Urea Bonds: Reversibility, Blocked Isocyanate, and Non-Isocyanate Polyurethane, *Chem. Rev.*, 2013, **113**, 80–118.
39 D. Liu, C. Huyan, H. Li, J. Ge, F. Chen and L. Zhang, Recycling and Upcycling of Polyurethane Thermosets: The Second Life of Polymers, *Adv. Mater.*, 2026, e15809, DOI: 10.1002/adma.202515809.
40 E. Balla, D. N. Bikiaris, N. Pardalis and N. D. Bikiaris, Toward Sustainable Polyurethane Alternatives: A Review of the Synthesis, Applications, and Lifecycle of Non-Isocyanate Polyurethanes (NIPUs), *Polymers*, 2025, **17**, 1364.
41 A. Gomez-Lopez, F. Elizalde, I. Calvob and H. Sardon, Trends in non-isocyanate polyurethane (NIPU) development, *Chem. Commun.*, 2021, **57**, 12254.
42 F. Orabona, F. Recupido, G. C. Lama, K. Polaczek, F. Taddeo, T. Salmi, M. Di Serio, L. Verdolotti and V. Russo, Cutting-edge development of non-isocyanate polyurethane (NIPU) foams: from sustainable precursors to environmental impact evaluation, *Green Chem.*, 2025, **27**, 7403.
43 C. Liang, U. R. Gracida-Alvarez, E. T. Gallant, P. A. Gillis, Y. A. Marques, G. P. Abramo, T. R. Hawkins and J. B. Dunn, Material Flows of Polyurethane in the United States, *Environ. Sci. Technol.*, 2021, **55**, 14215–14224.
44 N. G. Jaques, A. Llevot, É. Grau, T. Vidil, M. A. R. Meier and H. Cramail, High Molar Mass Non-Isocyanate Polyurethanes by Transurethanization of Diols with Isophorone-Based Bismethylcarbamate, *Macromol. Chem. Phys.*, 2025, **226**, 2500068.
45 F. C. Destaso, C. Libretti, C. L. Coz, E. Grau, H. Cramail and M. A. R. Meier, Optimized synthesis of a high oleic sunflower oil derived polyamine and its lignin-based NIPUs, *Green Chem.*, 2025, **27**, 1440.
46 J. Sawada, H. Sogawa, H. Marubayashi, S. Nojima, H. Otsuka, K. Nakajima, Y. Akae and T. Takata, Segmented Polyurethanes Containing Movable Rotaxane Units on the Main Chain: Synthesis, Structure, and Mechanical Properties, *Polymer*, 2020, **193**, 122358.
47 Y. Akae and P. Theato, Polyurethane Type Poly[3]rotaxanes Synthesized from Cyclodextrin Based [3]Rotaxane Diol and Diisocyanate, *Macromol. Rapid Commun.*, 2024, **45**, 2400441.
48 H. Sogawa, M. Abe, R. Shintani, T. Sotani, K. Tabaru, T. Watanabe, Y. Obora and F. Sanda, Polyurethanes containing platinum in the main chain: synthesis, structure and mechanofluorochromism, *Polym. J.*, 2023, **55**, 1119–1128.
49 P. Schara, A. M. Cristadoro, R. P. Sijbesma and Z. Tomovic, Solvent- Free Synthesis of Acetal-Containing Polyols for Use in Recyclable Polyurethanes, *Macromolecules*, 2023, **56**, 8866–8877.
50 Y. Akae, K. Iijima, M. Tanaka, T. Tarao and T. Takata, Main Chain-Type Polyrotaxanes Derived From Cyclodextrin-Based Pseudo[3]Rotaxane Diamine and Macromolecular Diisocyanate: Synthesis, Modification, and Characterization, *Macromolecules*, 2020, **53**, 2169–2176.
51 J. Futter, M. Holzer and B. Rieger, Formic Acid as Feedstock in the Phosgene-Free Dehydrogenative Coupling of Formamides and Alcohols to Polyurethanes, *Macromolecules*, 2025, **58**, 1817–1826.
52 Q. Jaussaud, I. M. Ogbu, G. G. Pawar, E. Grau, F. Robert, T. Vidil, Y. Landais and H. Cramail, Synthesis of polyurethanes through the oxidative decarboxylation of oxamic acids: a new gateway toward self-blown foams, *Chem. Sci.*, 2024, **15**, 13475.
53 T. Noda, A. Tanaka, Y. Akae and Y. Kohsaka, Unsaturated Polyurethanes Degradable by Conjugate Substitution Reactions With Amines and Carboxylate Anions, *RSC Adv.*, 2023, **13**, 20336–20341.
54 J. Lee, S. Baek, H. H. Moon, S. U. Son and C. Song, Furandiacylazide: A Biomass-Derived Versatile Polymer Platform toward Photodegradable and Nonflammable Polyurethanes, *ACS Appl. Polym. Mater.*, 2021, **3**, 5767–5777.
55 H. Tomita, F. Sanda and T. Endo, Model Reaction for the Synthesis of Polyhydroxyurethanes from Cyclic Carbonates with Amines: Substituent Effect on the Reactivity and

Selectivity of Ring-Opening Direction in the Reaction of Five-Membered Cyclic Carbonates with Amine, *J. Polym. Sci., Part A:Polym. Chem.*, 2001, **39**, 3678–3685.

56 S.-D. Lee, F. Sanda and T. Endo, A Novel Synthetic Method of a Polyurethane from an Aminimide as a "Latent Monomer", *J. Polym. Sci., Part A:Polym. Chem.*, 1997, **35**, 1333–1335.

57 S. Neffgen, H. Keul and H. Höcker, Cationic Ring-Opening Polymerization of Trimethylene Urethane: A Mechanistic Study, *Macromolecules*, 1997, **30**, 1289–1297.

58 L. Rubino, V. Patamia, A. Rescifina, M. Galimberti and V. Barbera, Cyclic carbamates based on (R)-(+)-limonene oxide for ring-opening polymerization, *Sci. Rep.*, 2024, **14**, 23521–21297.

59 D. Zhang, Y. Zhang, Y. Fan, M.-N. Rager, V. Gueŕineau, L. Bouteiller, M.-H. Li and C. M. Thomas, Polymerization of Cyclic Carbamates: A Practical Route to Aliphatic Polyurethanes, *Macromolecules*, 2019, **52**, 2719–2724.

60 E. A. Hoff, G. X. de Hoe, C. M. Mulvaney, M. A. Hillmyer and C. A. Alabi, Thiol–Ene Networks From Sequence-Defined Polyurethane Macromers, *J. Am. Chem. Soc.*, 2020, **142**, 6729–6736.

61 T. Mondal, L. Charles and J.-F. Lutz, Damage and Repair in Infor- mational Poly(N-Substituted Urethane)s, *Angew. Chem., Int. Ed.*, 2020, **59**, 20390–20393.

62 J. V. Hoorde, N. Badi and F. E. DuPrez, Scalable Design of Uni- form Oligourethanes for Impact Study of Chain Length, Sequence and End Groups on Thermal Properties, *Polym. Chem.*, 2024, **15**, 4319.

63 H. Yamauchi, S. Inayama, M. Nakabayashi and S. Hayashi, Sys- tematic Order-Made Synthesis of Sequence-Defined Polyurethanes With Length, Types, and Topologies, *ACS Macro Lett.*, 2023, **12**, 1264–1271.

64 W. Forysiak, A. Lizak and R. Szweda, Sequence of Monomers and Position of Stereocenters Matter for Thermal Properties of Stereocon- trolled Oligourethanes, *ChemPhysChem*, 2024, **25**, e202400366.

65 J. R. Sculuk, H. A. Fargher and E. V. Anslyn, The Utility of Chain-End Degradation for De Novo Sequencing of Sequence-Defined Oligourethanes, *Acc. Chem. Res.*, 2026, **59**, 958–968.

66 S. D. Dahlhauser, P. R. Escamilla, A. N. VandeWalle, J. T. York, R. M. Rapagnani, J. S. Shei, S. A. Glass, J. N. Coronado, S. R. Moor, D. P. Saunders and E. V. Anslyn, Sequencing of Sequence-Defined Oligourethanes via Controlled Self-Immolation, *J. Am. Chem. Soc.*, 2020, **142**, 2744–2749.

67 W. Forysiak, S. Kozub, Ł. John and R. Szweda, "Discrete oligourethanes of sequence-regulated properties – impact of stereocontrol, *Polym. Chem.*, 2022, **13**, 2980–2987.

68 A. Sharma, P. Cwynar, A. Jose, V. Gupta and R. Szweda, Step-economy approach for scalable synthesis of stereocontrolled and sequence-defined polyurethanes, *Eur. Polym. J.*, 2025, **236**, 114120.

69 Y. Akae, M. Sakurai and T. Takata, Alcohol Moiety-Tethering Acylazides as Versatile Isocyanate Precursors for Polymerization Initiators and Monomers, *Macromolecules*, 2021, **54**, 8488–8494.

70 Y. Akae and P. Theato, Polyurethanes by Ring-Opening Polymerization Initiated From Alcohol Moiety-Tethering Acylazide, *J. Polym. Sci.*, 2024, **62**, 4127–4135.

71 Y. Shen, P. Theato and Y. Akae, Tailored Polyurethane Synthesis from AB-Type Monomers, *Macromolecules*, 2024, **57**, 8162–8175.

72 J. Reeb, Y. Shen, P. Theato and Y. Akae, Controllable Photo-Degradability on Polyurethane From AB-Type Monomers, *Macromolecules*, 2025, **58**, 2701–2708.

73 X. Kneidl, L. Forkel, T. Cui, P. Theato and Y. Akae, The Effect of Aliphatic or Aromatic Substituents on the Synthesis and Properties of Polyurethanes From AB-Type Monomers, *J. Polym. Sci.*, 2026, **64**, 366–375.

74 D. V. Palaskar, A. Boyer, E. Cloutet, C. Alfos and H. Cramail, Synthesis of Biobased Polyurethane From Oleic and Ricinoleic Acids as the Renewable Resources via the AB-Type Self-Condensation Approach, *Biomacromolecules*, 2010, **11**, 1202–1211.

75 A. S. More, B. Gadenne, C. Alfos and H. Cramail, AB Type Polyaddition Route to Thermoplastic Polyurethanes From Fatty Acid Deriva- tives, *Polym. Chem.*, 2012, **3**, 1594.

76 A. S. More, L. Maisonneuve, T. Lebarbe, B. Gadenne, C. Alfos and H. Cramail, Vegetable-Based Building-Blocks for the Synthesis of Thermoplastic Renewable Polyurethanes and Polyesters, *Eur. J. Lipid Sci. Technol.*, 2013, **115**, 61–75.

77 C. Sivakumar and A. S. Nasar, Hydroxyl- and Amine-Terminated Hyperbranched Polyurethanes Using AB2-Type Azide Monomers: Synthesis, Characterization, Fluorescence, and Charge-Transfer Complexation Studies, *J. Polym. Sci., Part A: Polym. Chem.*, 2009, **47**, 3337–3351.

78 T. Shioiri, K. Ishihara and M. Matsui, Cutting Edge of Diphenyl Phosphorazidate (DPPA) as a Synthetic Reagent – A Fifty-Year Odyssey, *Org. Chem. Front.*, 2022, **9**, 3360.

79 Y. Akae, J. Sawada, K. Nakajima and T. Takata, The Effect of the Axle End Structure and Number of Through-Space Bonds on the Properties of Rotaxane Crosslinked Polymers, *Angew. Chem., Int. Ed.*, 2023, **62**, e202303341.

80 Y. Akae, H. Sogawa and T. Takata, Effective Synthesis and Modification of α-Cyclodextrin Based [3]Rotaxanes Enabling Versatile Molecular Design, *Eur. J. Org. Chem.*, 2019, **22**, 3605–3613.

81 Y. Akae, H. Sogawa and T. Takata, Evaluation of Induced Circular Dichroism via Through Space Chirality Transfer in alpha-Cyclodextrin-Based Rotaxanes Directed toward Fine Tuning, *Bull. Chem. Soc. Jpn.*, 2019, **92**, 1413–1418.

82 T. Shioiri, K. Ninomiya and S. Yamada, Diphenylphosphoryl Azide. New Convenient Reagent for a Modified Curtius Reaction and for Peptide Synthesis, *J. Am. Chem. Soc.*, 1972, **94**, 6203–6205.

83 See ESI.

84 Y. Akae, H. Okamura, Y. Koyama, T. Arai and T. Takata, Selective Synthesis of a [3]Rotaxane Consisting of Size-

Complementary Components and Its Stepwise Deslippage, *Org. Lett.*, 2012, **14**, 2226–2229.

85 Y. Akae, Y. Koyama, S. Kuwata and T. Takata, Cyclodextrin-Based Size-Complementary [3]Rotaxanes: Selective Synthesis and Specific Dissociation, *Chem. – Eur. J.*, 2014, **20**, 17132–17136.

86 Y. Akae, H. Sogawa and T. Takata, Synthesis of a Structure Definite α-Cyclodextrin Based Macromolecular [3]Rotaxane Using a Size-Complementary Method, *Angew. Chem., Int. Ed.*, 2018, **57**, 11742–11746, (*Angew. Chem.*, 2018, **130**, 11916–11920).

87 O. Shelef, S. Gnaim and D. Shabat, Self-Immolative Polymers: An Emerging Class of Degradable Materials With Distinct Disassem- bly Profiles, *J. Am. Chem. Soc.*, 2021, **143**, 21177–21188.

88 R. E. Yardley, A. R. Kenaree and E. R. Gilles, Triggering Depolym- erization: Progress and Opportunities for Self-Immolative Polymers, *Macromolecules*, 2019, **52**, 6342–6360.

89 G. I. Peterson, M. B. Larsen and A. J. Boydston, Controlled Depolymerization: Stimuli-Responsive Self-Immolative Polymers, *Macromolecules*, 2012, **45**, 7317–7328.